APPENDICES

APPENDIX A: Theoretical Background

The Theory of Quantum Chemical Calculations

The quantum mechanical methods are based on solving the time independent Schrödinger wave equation and are used to determine the electronic structures of atom and molecules. They can be divided into two categories: *ab initio* and semiempirical methods. *Ab initio* methods such as Hartree-Fock (HF) or molecular orbital (MO) theory, configuration interaction (CI) theory, perturbation theory (PT), and density functional theory (DFT) can have accuracy in structure and energy predictions when compared with experimental. However, the weak point of *ab initio* calculations is extremely demanding in computer resources, especially for large molecular systems. Semiempirical quantum chemical methods lie between *ab initio* and molecular mechanics (MM). Like MM, they use experimentally derived parameters to strive for accuracy; like *ab initio* methods, they are quantum-mechanical in nature. Semiempirical methods are computationally fast because many integrals neglected. The error is compensated through the use of experimentally derived parameters. Table A1 attempts to show the advantages and the disadvantages of MM, semiempirical and *ab initio* methods.

Appendix Table A1 Synopsis of molecular calculations.

Method	Advantages	Disadvantages	Best for
Ab initio -Uses quantum physics -Mathematically rigorous: no empirical parametes	-Useful for a broad range of systems -Are not depend on experimental data -Transition states and excited states can be calculated.	-Computationally expensive	-Small systems -Electronic transitions -Systems requiring high accuracy.
Semi-empirical -Uses quantum physics -Uses experimental parameters -Uses extensive approximations	-Less demanding computationally than *ab initio* methods. -Calculates transition states and excited states.	-Requires *ab initio* results or experimental data for parameters. -Less rigorous than *ab initio* methods.	-Medium-sized systems (hundreds of atoms). -Electronic transitions.
Molecular Mechanics -Uses classical physics -Relies on force field with embedded empirical parameters.	-Computationally 'cheap', fast and useful with limited computer resources. -Can be used for biomolecules and biomolecule complexes.	-Electronic properties are not Calculated. -*Ab initio* or experimental data for parameters are required.	-Large systems (thousands of atoms) and more -System or processes that do not involve bond breaking.

The time independent Schrödinger equation for a molecule (n-electron and N-nuclei system) is

$$H\Psi(\vec{r},\vec{R}) = E\Psi(\vec{r},\vec{R}) \tag{20}$$

The molecular wavefunction, $\Psi(\vec{r},\vec{R})$, depends on the coordinates of all electrons in the system (r) and nuclear coordinates (R). When the wave function (Ψ) is known, all physical observables of interest can be calculated.

Mostly, the time-independent Schrödinger equation is too complicate to be solved directly. Consequently, approximations have to be introduced to make calculations of various molecular properties possible. The Born-Oppenheimer approximation is the assumption that the electronic motion and the nuclear motion in molecules can be separated as shown in equation (21).

$$\Psi\left(\vec{r},\vec{R}\right) = \psi_{elec}\left(\vec{r},\vec{R}\right)\psi_{nucl}\left(\vec{R}\right) \tag{21}$$

where H is Hamiltonian operator (in atomic units) which compose of the kinetic operator, T, and potential operator, V, that is;

$$H = T + V$$

$$H = -\sum_{i=1}^{N}\frac{1}{2}\nabla_i^2 - \sum_{A=1}^{M}\frac{1}{2M_A}\nabla_A^2 - \sum_{i=1}^{N}\sum_{A=1}^{M}\frac{Z_A}{r_{iA}} + \sum_{i=1}^{N}\sum_{j>i}^{N}\frac{1}{r_{ij}} + \sum_{A=1}^{M}\sum_{B>A}^{M}\frac{Z_A Z_B}{R_{AB}} \tag{22}$$

where the Laplacian operator, ∇^2, is ;

$$\nabla^2 = \frac{\partial^2}{\partial x^2} + \frac{\partial^2}{\partial y^2} + \frac{\partial^2}{\partial z^2}$$

$$T = -\frac{\hbar^2}{2m}\nabla^2$$

The motion of the nuclei is separated out from the motion of the electrons. Equation (22) can be rewritten as

$$\mathrm{H} = -\sum_{A=1}^{M}\frac{1}{2M_A}\nabla_A^2 + \mathrm{H}_{el} \tag{23}$$

The electronic wavefunction depends upon the nuclear positions but not upon their velocities, i.e., the nuclear motion is so much slower than electron motion that they can be considered to be fixed. Thus, the nuclear-nuclear repulsion term (the final in equation (22)) appears as a constant in H_{el}. From (21), (22) and (23) can obtain;

$$\mathrm{H}\Psi(\vec{r},\vec{R}) = \mathrm{H}\psi_{elec}(\vec{r},\vec{R})\psi_{nucl}(\vec{R}) = \left(-\sum_{A=1}^{M}\frac{1}{2M_A}\nabla_A^2 + \mathrm{H}_{el}\right)\psi_{elec}(\vec{r},\vec{R})\psi_{nucl}(\vec{R})$$

$$= \left(-\sum_{A=1}^{M}\frac{1}{2M_A}\nabla_A^2 + \mathrm{E}_{el}\right)\psi_{elec}(\vec{r},\vec{R})\psi_{nucl}(\vec{R}) = \mathrm{E}\psi_{elec}(\vec{r},\vec{R})\psi_{nucl}(\vec{R}) = \mathrm{E}\psi \tag{24}$$

The nuclear wave function, ψ_{nucl}, describes the vibrational, rotational and translational motion of the nuclei.

The influence of the nuclear derivative on the electron wave function (ψ_{el}) is considered that neglect (i.e. the nuclei move slowly compared with the electrons) Thus equation (24) can be separated into two equations, an electronic part:

$$\mathrm{H}_{el}\psi_{el}(\vec{r},\vec{R}) = \mathrm{E}_{el}(\vec{R})\psi_{el}(\vec{r},\vec{R}), \tag{25}$$

where

$$H_{el} = -\sum_{i=1}^{N} \frac{1}{2} \nabla_i^2 - \sum_{i=1}^{N} \sum_{A=1}^{M} \frac{Z_A}{r_{iA}} + \sum_{i=1}^{N} \sum_{j>i}^{N} \frac{1}{r_{ij}} + \sum_{A=1}^{M} \sum_{B>A}^{M} \frac{Z_A Z_B}{R_{AB}}, \quad (26)$$

and a nuclear part:

$$H_{nucl} \psi_{nucl}(\vec{R}) = E \psi_{nucl}(\vec{R}), \quad (27)$$

where

$$H_{nucl} = -\sum_{A=1}^{M} \frac{1}{2M_A} \nabla_A^2 + E_{el}(\vec{R}) \quad (28)$$

Some of the computational approaches have been used to solve the Schrödinger equation. To make the computations feasible, some approximations are used. There are two main procedures, ab initio calculation and semiempirical methods to solve the Schrödinger equation. In an initio calculations, a model is chosen for the electronic wavefunction and equation (20) is solved using the values of the fundamental constants and atomic number of nuclei as input. The accuracy of this approach depends on the model chosen for wavefunction. For large molecules, accurate ab initio calculations are computationally expensive. Thus, semiempirical methods have been developed to treat such large molecules. Semiempirical methods make use of a simiplified form for the Hamiltonian and adjustable parameter obtained from experimental data.

1. The Hartree Fock approach

The starting point of many *ab initio* quantum chemistry methods is Hartree-Fock method. The third term ($\frac{1}{r_{ij}}$) in equation (26) is the crucial complication in all electronic structure calculations. This complication can be neglected by assuming that

the electrons are non-interacting. This implies that the n-electron equation can be separated into n one-electron equations.

$$\mathrm{H}_{el} = \sum_{i=1}^{N} h(i) \tag{29}$$

$$h(i) = \left(-\frac{1}{2}\nabla_i^2 - \sum_{A=1}^{M} \frac{Z_A}{r_{iA}} \right), \tag{30}$$

where h(i) is the core Hamitonian for electron i. The total wavefunction is product of one-electron wavefunctions:

$$\psi = \psi_a(1)\psi_b(b)...\psi_z(n) \tag{31}$$

The electronic wavefunction must obey the Pauli principle so the electron spin is taken into account. The products of the spatial orbitals and the spin functions ($\alpha(\omega)$ and $\beta(\omega)$) is called spin orbitals, $\phi_i(i)$. The overall wavefunction is written in terms of a Slater determinant, which has the antisymmetric properties:

$$\psi = (n!)^{-1/2} \begin{vmatrix} \phi_a(1) & \phi_b(1) & \cdots & \phi_z(1) \\ \phi_a(2) & \phi_b(2) & & \\ \cdots & & \cdots & \\ \phi_a(n) & \phi_b(n) & \cdots & \phi_z(n) \end{vmatrix} \tag{32}$$

which commonly is written like:

$$|\psi\rangle = (n!)^{-1/2} |\phi_a(1), \phi_b(2), ..., \phi_z(n)\rangle \tag{33}$$

The pre-factor $(n!)^{-1/2}$ is a normalisation constant, and the $\{\phi_i\}$ are assumed orthonormal.

A product wavefunction of equation (33) is sought, with the electron-electron repulsions treaed in an average way. Each electron is considered to be moving in the electrostatic field of the nuclei and average field of the other n-1 electrons. The spin orbitals are found by using variation theory which involves minimizing the Rayleigh ratio.

$$\mathrm{E}_e = \frac{\langle \psi | \mathrm{H}_e | \psi \rangle}{\langle \psi | \psi \rangle} \geq \mathrm{E}_{exact} \tag{34}$$

E_e is identifined with the electronic energy of ground state of the atom and molecule for the selected nuclear configuration R.

The application of this minimization procedure leads to Hartree Fock equation for the individuals spinorbitals. The Hartree-Fock equation for spinorbital is,

$$f_1 \phi_a(1) = \varepsilon_a \phi_a(1)\,, \tag{35}$$

where ε_a is the spinorbital energy and f_1 is the Fock operator:

$$f_1 = h_1 + \sum_u \{J_u(1) - K_u(1)\}, \tag{36}$$

where h_1 is the core Hamiltonian for electron 1. The Coulomb operator, J_u, and exchange operator, K_u, are defined here in term of spin orbitals as follows:

$$J_u(1)\phi_a(1) = j_0 \left\{ \int \phi_u^*(2) \frac{1}{r_{12}} \phi_u(2)\, dx_2 \right\} \phi_a(1) \tag{37}$$

$$K_u(1)\phi_a(1) = j_0\left\{\int \phi_u^*(2)\frac{1}{r_{12}}\phi_a(2)dx_2\right\}\phi_u(1) \tag{38}$$

$$j_0 = \frac{e^2}{4\pi\varepsilon_0}$$

$$f_1 = h_1 + \sum_u \{J_u(1) - K_u(1)\} \tag{39}$$

The Coulomb operator take into account the Coulombic repulsion between electrons, and the exchange operator represent the effects of spin correlation. The sum in equation (39) represents the average potential energy of electron 1 due to the presence of the other n-1 electrons. HF equations are solved by self-consistent procedure, a trial set of spin orbitals is formulated and used to construced the Fock operator, then HF equation are solved to obtain a new set of spin orbitals which are used to construct a new Fock operator. The cycle of calculation is repeated until a convergence criterion is satisfied (Appendix Figure A1). However, the solution for spin orbitals for molecular system is computationally complex. Thus C.C.J. Rothaan and G.G. Hall suggested using a known set of basis functions with which to expand the spin orbitals. For the restricted closed shell, the Hartree-Fock equation for the spatial function ψ_a(a) occupied by electron 1 is

$$f_1\psi_a(1) = \varepsilon_a\psi_a(1)\ , \tag{40}$$

where f_1 is the Fock operator expressed in terms of spatial wavefunction:

$$f_1 = h_1 + \sum_u \{2J_u(1) - K_u(1)\} \tag{41}$$

Each spatial wavefunction ψ_i is a linear combination of basis function ϕ_j:

$$\psi_i = \sum_{j=1}^{M} c_{ji}\phi_j \,, \tag{42}$$

where c_{ji} are unknown coefficients. The problem of calculating the wave function has been transformed to computing of the coefficients. When equation (42) is substituted into equation (40), equation (43) is obtained.

$$f_1 \sum_{j=1}^{M} c_{ja}\phi_j(1) = \varepsilon_a \sum_{j=1}^{M} c_{ja}\phi_j(1) \tag{43}$$

Multiplication of the both sides of equation (43) by ϕ_i^* and integration over r_1. We can get equation (44).

$$\sum_{j=1}^{M} c_{ja} \int \phi_i^*(1) f_1 \phi_j(1) dr_1 = \varepsilon_a \sum_{j=1}^{M} c_{ja} \int \phi_i^*(1)\phi_j(1) dr_1 \tag{44}$$

S, the overlap matrix, and F, the Fock matrix, are defined as equation (45) and (46), respectively.

$$S_{ij} = \int \phi_i^*(1)\phi_j(1) dr_1 \tag{45}$$

$$F_{ij} = \int \phi_i^*(1) f_1 \phi_j(1) dr_1 \tag{46}$$

The equation (44) becomes

$$\sum_{j=1}^{M} F_{ij} c_{ja} = \varepsilon_a \sum_{j=1}^{M} S_{ij} c_{ja} \tag{47}$$

Equation (44) can be rewritten in matrix form:

$$FC = SC\varepsilon \,, \tag{48}$$

where c is and MxM matrix consiste of elements c_{ja} and ε is an MxM diagonal matrix of the orbital energies. This equation can not be solved directly because the matrix element F_{ij} involve integrals over the Coulomb and exchange operators which themselves depend on the spatial wavefunctions. The self consistent field approach is used to solve equation (48).

$$F_{ij} = h_{ij} + \sum_{l,m} P_{lm}\left[(ij|lm)\right] - \frac{1}{2}(im|lj), \tag{49}$$

where h_{ij} , core-Hamiltonian matrix, is defined as

$$h_{ij} = \int \phi_i^*(1) h(1) \phi_j(1) dr_1 \tag{50}$$

The matrix P is the density matrix or charge- and bond-order matrix,

$$P_{lm} = 2\sum_u C_{lu}^* C_{mu} \tag{51}$$

When $l=m$, P_{ll} is the electron density on atom; when $l \neq m$, P_{lm} is the bond order between l and m. The term $(ij|lm)$ in Equation (49) signified the two-electron repulsion integrals, defined as

$$(ij|lm) = \int dr_1 dr_2 \phi_i^*(1) \phi_j(2) r_{12}^{-1} \phi_l^*(2) \phi_m(2) \tag{52}$$

Two electron integral was considered to be one of the greatest problem in quantum chemistry, but the one-electron matrix elements h_{ij} is evaluated only once because they remain unchanged during each iteration, but P_{lm} needs to be re-evaluated at each iteration.

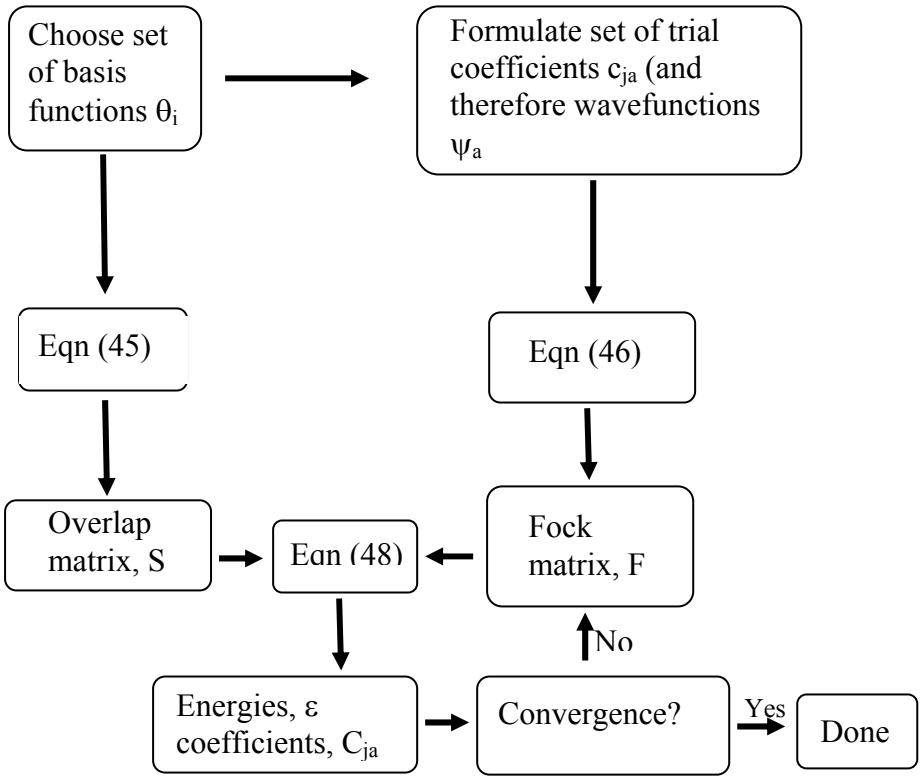

Appendix Figure A1 A Summary of the iteration procedure for a Hartree-Fock self-consistent field calculations.

Source : Atkins (2005)

2. Basis Set

A complete set of basis function is used to represent spin orbitals exactly. The use of an infinite number of basis functions is not computationally feasible, a finite basis set is always used and the error due to the imcompleteness of basis is called the basis-set truncation error. A critical computational is to keep the number of basis function low and to choose them cleverly. The basis set used in quantum mechanical calculations are composed of atomic functions. The approximation involves expressing the molecular orbitals as linear combinations of set of one-electron functions known as basis function. An individual molecular orbitals is defined as:

$$\phi_i = \sum_{\mu=1}^{N} c_{\mu i}\chi_\mu \ , \tag{53}$$

where the coefficients $c_{\mu i}$ are known as molecular orbital expansion coefficients. The basis function $\chi_1 ... \chi_N$ are also chosen to be normalized. A complete basis set consists of STOs with all permitted integral values of n, l, and m_l and all positive values of the orbital exponents, ζ (zeta). STO basis functions are centered on the atomic nucleus. For diatomic and polyatomic species, STOs are centered on each of the atoms. However, the evaluation of the many two-electron integrals in molecules with three and more atom is impractical for STOs. Therefore, Gaussian-type orbitals are introduced by S.F Boys in 1950. They play a major role in ab initio calculations to make then computationally feasible. Gaussian functions have the general form:

$$g(\alpha, \vec{r}) = cx^n y^m z^l e^{-\alpha r^2} \ , \tag{54}$$

where $\vec{r}$ is of course composed of x, y, and z. α is a constant determining the size (radical extent) of the function. When n=m=l=0, the Cartesian Gaussian is an s-type Gaussian; when n+m+l=1, it is a p-type Gaussian; when n+m+l=2, it is a d-type Gaussian, and so on. In Gaussian function, $e^{-\alpha r}$ is multiplied by powers (possibly 0) of x, y, and z and a constant for normalization, so that:

$$\int_{allspace} g^2 = 1 \tag{55}$$

Thus, c depends on α, l, m, and n.

Here are three representative Gaussian functional (s, p_y and d_{xy} types, respectively):

$$g_s(\alpha,\vec{r}) = \left(\frac{2\alpha}{\pi}\right)^{3/4} e^{-\alpha r^2}$$

$$g_y(\alpha,\vec{r}) = \left(\frac{128\alpha^5}{\pi^3}\right)^{1/4} y e^{-\alpha r^2}$$

$$g_{xy}(\alpha,\vec{r}) = \left(\frac{2048\alpha^7}{\pi^3}\right)^{1/4} xy e^{-\alpha r^2} \qquad (56)$$

The advantage of GTOs is much easier to compute, but GTOs does not cusp while STO has cusp. To alleviate this problem, several GTOs are grouped together to form what are known as contracted Gaussian functions. Each contracted Gaussian functions(χ_j) are linear combinations of primitive Gaussians(g_i) like these are used to form the actual basis functions; the contracted Gaussians have the form:

$$\chi_j = \sum_P d_{ji} g_i \,, \qquad (57)$$

where the d_{ji}'s are fixed constants within a given basis set. Note that contracted functions are also normalized in common practice. The use of contracted Gaussian functions reducing the number of coefficient c_{ji} to be in HF calculation leads to large saving in computer time with litlle loss of accuracy if the contracted Gaussians are well-chosen. The spatial orbitals are then expressed as a linear combination of the contracted Gaussians:

$$\psi_i = \sum_j c_{ij} \chi_j \qquad (58)$$

The simplest type of basis set is a minimal basis sets in which one function is used to represent each of the orbitals of elementary valence theory. For example, a minimal basis set for H_2O consists of seven functions, two basis functions to represent the two H1s orbitals and five functions to represent the 1s-, 2s-, $2p_x$-, $2p_y$, $2p_z$-orbital of oxygen. However, a minimal basis set results in wavefunctions and energies that are

not very close to the Hartree-Fock limit.

Split Valence Basis Sets

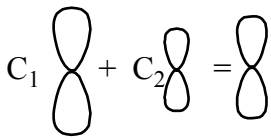

In split valence basis set, each atomic orbital is represented by two basis functions while each inner-shell atomic orbital is represented by a single basis function. For example, hydrogen and carbon are represented as:

H: 1s, 1s'

C: 1s, 2s, 2s', $2p_x$, $2p_y$, $2p_z$, $2p'_x$, $2p'_y$, $2p'_z$

In the (9s5p)/[3s2p] contraction sheme, nine s-type and five p-type primitive Gaussians are contracted into three (one basis function for 1s and two basis function for valence 2s-orbital) and two basis functions (two for each of the each of the three 2p-orbitals), respectively. Therefore, the contraction scheme reduces the total number of basis functions from 24 (five p-type primitives for each of $2p_x$, $2p_y$ and $2p_z$) to nine. This reduction achieves decrease in computer time because the number of two-electron integrals to be evaluated is proportional to the fourth power of the number of basis functions.

Polarized Basis Sets

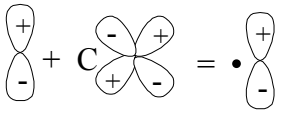

Split valence basis sets allow orbitals to change size, but not to change shape. Polarized basis sets remove this limitation by adding orbitals with angular momentum

beyond what is required for the ground state to the description of each atom. For example, polarized basis sets add d functions to carbon atoms and f functions to transition metals, and some of them add p functions to hydrogen atoms.

So far, the only polarized basis set 6-31G(d) is used. Its name indicates that it is the 6-31G basis set with d functions added to heavy atoms. This basis set is becoming very common for calculations involving up to medium-sized systems. This basis set is also known as 6-31G*. Another popular polarized basis set is 6-31G(d,p), also known as 6-31G**, which adds p functions to hydrogen atoms in addition to the d functions on heavy atoms.

Diffuse Functions

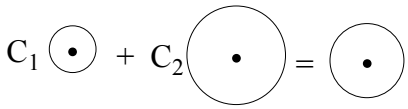

Diffuse functions are large-size versions of s- and p- type functions (as opposed to the standard valence-size functions) which allow orbitals to occupy a larger region of space. Basis sets with diffuse functions are important for systems where electrons are relatively far from the nucleus: molecules with lone pairs, anions and other systems with significant negative charge, systems in their excited states, systems with low ionization potentials, descriptions of absolute acidities. The 6-31+G(d) basis set is the 6-31G(d) basis set with diffuse functions added to heavy atoms. The double plus version, 6-31++G(d), adds diffuse functions to the hydrogen atoms as well. Diffuse functions on hydrogen atoms seldom make a significant difference in accuracy.

High Angular Momentum Basis Sets

Even larger basis sets are now practical for many systems. Such basis sets add multiple polarization functions per atom to triple zeta basis set. For example, the 6-31G(2d) basis set adds two d functions per heavy atom instead of just one, while the

6-311++G(3df,3pd) basis set contains three sets of valence region functions, diffuse functions on both heavy atoms and hydrogens, and multiple polarization funtions:3 d functions and 1 f function on heavy atoms and 3 p functions and 1 d function on hydrogen atoms. Such basis sets are useful for describing the interactions between electrons in electron correlation methods.

3. Electron correlation

The HF ground state wavefunction is not the exact wavefunction, and it does not consider the instantaneous Coulombic interaction between electrons. Thus the HF method ignores electron correlation. A great deal of modern work in the field of electron structure calculation is aimed at taking electron correlation into account.

The HF method yields a finite set of spinorbitals when a finite basis set expansion is used. In general, a basis with M members results in M spatial wavefunction and 2M different spinorbitals. Many Slater determinants can be formed from 2M different spinorbitals by promoting many electrons from occupied orbitals to virtual orbitals. The difference between exact energy and HF limit is called the correlation energy.

3.1 Configuration interaction (CI)

The exact ground-state or exited-state wavefunction can be assumed as linear combination of all possible n-electron Slater determinants arising from a complete set of spinorbitals. Therefore, the exact electronic wavefunction Ψ for any state of the system can be written in the form

$$\Psi = C_0\Phi_0 + \sum_{a,p} C_a^p \Phi_a^p + \sum_{\substack{a\prec b \\ p\prec q}} C_{ab}^{pq} \Phi_{ab}^{pq} + \ldots \qquad (59)$$

CI accounts for the electron correlation neglected in the Hartree Fock method. CI is popular method for the calculation of accurate molecular wavefunction and potential

energy surface, and it is variational. The limited CI calculations are the lack of size-consistency. In configuration interaction calculation, the ground –or excited-state wave function,Ψ, for state s is represented as a linear combination of n-electron Slater determinants (equation 60).

$$\Psi_s = \sum_{J=1}^{L} C_{js} \Phi_j \tag{60}$$

where the sum is taken over a finite number L of determinants Φ_j with expansion coefficients C_{js} for the state s. The expansion coefficients C_{js} are determined variationally by minimizing the Rayleigh ratio using Ψ_s as the trial function.

3.2 Moller-Plesset many-body perturbation theory

One important feature of CI is that it is variational but one disadvantage is Its lack of size-consistancy. Purturbation theory provides an alternative systematic approach to finding the correlation: whereas its calculations are size consistent, they are not variational in that it does not in general give energies that are upper bounds to the exact energy. The application of PT to system composed of many interacting particle is called many-body perturbation theory (MBPT).

The zero-order Hamiltonian $H^{(0)}$ in MPPT, is the sum of the one-electron Fock operators defined in equation (61).

$$H^0 = H_{HF} = \sum_{i=}^{n} f_i \tag{61}$$

The HF ground-state wavefunction Φ_0 is an eigenfunction of H_{HF} and that its eigenvalue equals the sum of the occupied spinorbitals energies. The perturbation $H^{(1)}$ is given by

$$H^{(1)} = H - \sum_{i=}^{n} f_i \tag{62}$$

The HF energy E_{HF} associated with the ground-state HF wave function Φ_0 is the expectation value.

$$E_{HF} = \left\langle \Phi_0 \middle| H_{HF} + H^{(1)} \middle| \Phi_0 \right\rangle \tag{63}$$

It is easy to show that E_{HF} is equal to the sum of the zero-order energy $E_0^{(0)}$ and the first-order energy correction $E_0^{(1)}$

$$E_{HF} = E_0^{(0)} + E_0^{(1)} \tag{64}$$

Therefore, the first correction to the ground-state energy is given by second order perturbation theory as

$$E^{(2)} = \frac{1}{4} \sum_{a,b}^{occ} \sum_{p,q}^{vir} \frac{\langle ab \| pq \rangle \langle pq \| ab \rangle}{\varepsilon_a + \varepsilon_b - \varepsilon_p - \varepsilon_q} \tag{65}$$

where

$$\langle ab \| pq \rangle = j_0 \int \phi_a^*(1) \phi_b^*(2) \frac{1}{r_{12}} \phi_p(1) \phi_q(2) dx_1 dx_2 - j_0 \int \phi_a^*(1) \phi_b^*(2) \frac{1}{r_{12}} \phi_q(1) \phi_p(2) dx_1 dx_2 \tag{66}$$

ϕ_a and ϕ_b are occupied spin orbitals and ϕ_p and ϕ_q are virtual spin orbitals. The second-order energy correction in MPPT is called MP2. In general, Bond lengths of bonds involving hydrogen computed using MP2 are in good agreement with experimental. The third- and fourth-order energy corrections are denoted MP3 and MP4. The higher orders of perturbation theory are second more complicated.

3.3 The coupled-cluster method

Another popular *ab initio* method, like MPPT, is size-consistent but not variational, it is called the coupled-cluster method. The CC method introduces the cluster operator C, which relates the exact electronic wavefunction Ψ to the HF wavefunction Φ_0

$$\Psi = e^C \Phi_0, \tag{67}$$

where the exponectial operator e^C is

$$e^C = 1 + C + \frac{1}{2!}C^2 + \frac{1}{3!}C^3 + \ldots \tag{68}$$

The effect of the cluster operator C on Φ_0 is to give a linear combination of slater determinants in which electrons from occupied spinorbitals have been excited to virtual spinorbitals. In particular, C is the sum of the one electron excitation operator C_1, two-electron excitation operator C_2,…, N-electron excitation operator C_N The effects of the excitation operators are

$$C_1 \Phi_0 = \sum_{a,p} t_a^p \Phi_a^p \tag{69}$$

$$C_2 \Phi_0 = \sum_{a,p} t_{ab}^{pq} \Phi_{ab}^{pq} \tag{70}$$

and likewise for C_3 to C_N; the t_a^p are called single-excitation amplitudes, t_{ab}^{pq} double-excitation amplitudes, and so on. Two approximations are widely made in CC applications. First, a finite basis set is used in the determination of Φ_0. Second, the expression for the cluster operator C is truncated to include only specified electron excitation operators.

4. Density Functional Theory

The ab initio methods start with the Hartree-Fock approximation in that HF equations are first solved to find spinorbitals that can then be used to construct configuration state functions. They have limitations. The accurate calculations with large basis sets on molecules containing many atom and many electrons is difficult to perform. Density functional theory (DFT) is popular among quantum chemists. DFT begin with the concept of the electron probability density. One reason for the popularity of DFT is that it takes into account electron correlation while being less demanding computationally than, for example, CI and MP2. It can be used to do calculations on molecules of 100 or more atoms closely with experiments than HF calculations. The electronic energy E is functional of electron density and is denoted E(ρ).

In fact the algorithms of the approach, in which the electron density is described in terms of one-electron basis functions, are very similar to the single-determinant HF algorithm. While the concept of expressing part or all of the molecular energy as a functional of the electron density goes back to the early days of quantum theory, Density Functional Theory (DFT) was put on a rigorous theoretical foundation by the Hohenberg-Kohn theorem. It states that there exists unique density ρ that yield the exact ground energy of system. The subsequent work of Kohn and Sham laid the basis for practical computational applications of the DFT to real systems. W. Kohn and L. J. Sham showed that the exact ground state electronic energy E of an n-electron system can be written as

$$E(\rho) = -\frac{\hbar^2}{2m_e}\sum_{i=1}^{n}\int \psi_i^*(r_1)\nabla_1^2\psi_i(r_1)dr_1 - j_0\sum_{I=1}^{N}\frac{Z_I}{r_{I1}}\rho(r_1)dr_1 + \frac{1}{2}j_0\int\frac{\rho(r_1)\rho(r_2)}{r_{12}}dr_1dr_2 + E_{XC}[\rho], \tag{71}$$

where the one-electron spatial orbital ψ_i(i=1, 2,…,n) are the Kohn-Sham orbitals. The exact ground-state electron density is given by

$$\rho(r) = \sum_{i=1}^{n} |\psi_i(r)|^2 , \tag{72}$$

where the sumation is done over all the occupied Kohn-Sham (KS) orbitals; ρ is known. The first term on the right in equation (71) represents the kinetics energy of electrons; the second term represents the electron-nucleus attraction where the sum is over all N nuclei with index I and atomic number Z_I; the third term represents the Coulomb interaction between the total charge distribution at r_1 and r_2; the last term is the exchange-correlation energy of the system, which is also a functional of the density and takes into account all non-classical electron-electron interactions. One of the four terms, E_{XC} is not known how to be obtained exactly. The KS orbitals are found by solving the Kohn-Sham equations, which are derived by applying the variational principle to the electronic energy E(ρ) with the charge density given by equation (72). The KS equations for the one-electron orbitals $\psi_i(r_1)$

$$\left\{ -\frac{\hbar^2}{2m_e}\nabla_1^2 - j_0 \sum_{I=1}^{N} \frac{Z_I}{r_{I1}} + j_0 \int \frac{\rho(r_2)}{r_{12}} dr_2 + V_{XC}(r_1) \right\} \psi_i(r_1) = \varepsilon_i \psi_i(r_1) , \tag{73}$$

where ε_i are the KS orbital energies and exchange-correlation potential, V_{XC}, is the function derivative of the exchange-correlation energy. The KS equation is solved by a self consistent fashion. Stating with the electron density is guessed by using superposition of atomic densities. Next V_{xc} as function of *r* is computed. The set of KS equations is then solved to obtain an initial set of KS orbitals. This set of orbitals is then used to compute an improved density from equation (72), and the process is repeated until the density and exchange-correlation energy have converged. Then the electronic energy is computed from eqation (71). The computational time required for a DFT calculation scale as the third power of the number of basis functions. Therefore, DFT methods are computationally more efficient than HF method.

4.1 Exchange-correlation functionals

The obtaining approximate forms for the functional for the exchange-correlation energy have been developed. This functionals are often separated into an exchange functional (representing exchange energy) and a correlation functional (representing dynamic correlation energy).

$$E_{XC}(\rho) = E_X(\rho) + E_C(\rho) \tag{74}$$

In the local density approximation (LDA), the exchange correlation functional is

$$E_{XC}(\rho) = \int \rho(r)\varepsilon_{XC}[\rho(r)]dr \tag{75}$$

This equation is an approximation for gas with constant density. However, the accuracy of this method decreases with varying electon density in the system and many molecules, In LDA, the exchange functional and correlation functional depend only on ρ but not on any derivatives of ρ. Therefore, to account for the inhomogeneity of electron density, a non-local correction involving the gradient of ρ is often added to the exchange-correlation energy given in equation (73). Thus the LDA with gradient corrections is called the generalized approximation (GGA).

A variety of exchange-correlation functionals such as B3LYP, BLYP, BP91 and PBE have been developed for use in DFT calculations. For example, the popular B3LYP functional is a combination of the gradient-corrected exchange functional developed by A.D. Becke and the gradient-corrected correlation functional developed by C. lee, W. Yang, and R.G. Parr. Some of the functional such as B3LYP represent hybrid DFT calculations that use the Hartree-Fock correction in conjunction with density functional correlation and exchange. The B3LYP functional looks like this:

$$E_{XC}^{B3LYP} = a_{X0}E_X^S + (1-a_{X0})E_X^{HF} + a_{X1}\Delta E_X^B + E_C^{VWN} + a_C\Delta E_C^{LYP} \tag{76}$$

where $a_{X0} = 0.80$, $a_{X1} = 0.72$ and $a_C = 0.81$, which are values fitted for a selected set of molecules to reproduce the heat of formation. The term E_X^{HF} is calculated using the Kohn-Sham orbitals in the manner of the HF procedure by computing the exchange integrals. The B3LYP functional often uses $\Delta E_C^{3LYP} = E_C^{LYP} - E_C^{VWN}$.

5. Semi-empirical Calculations

Ab initio methods were not be applied routinely to molecules with several dozen atoms, but semiempirical methods are fast enough to treat also larger systems. Ab initio represent a more theoretically pure approach. Semiempirical methods use many approximation and neglection, which are compensated by a parametization using experimental data.

In semiempirical methods, valence electrons are treated only while the core electrons are included in the nuclear core. Moreover, two-electron integrals are set to zero in the treatment. The main implication of this is that the Roothaan-Hall equations are simplified: FC = CE. The valence-electron Hamitonian H_v for a closed-shell molecule with n_v valence electrons is

$$H_V = \sum_{i=1}^{n_V} h_i^V + \frac{1}{2} j_0 \sum_{i,j}^{n_V} \frac{1}{r_{ij}}, \tag{77}$$

where h_i^V is the core Hamiltonian for valence electron *i* given by

$$h_i^V = -\frac{\hbar^2}{2m_e} \nabla_1^2 + V_i^{V,eff} \tag{78}$$

and $V_i^{V,eff}$ is the effective potential energy for valence electron i resulting from the potential filed of the nuclei and all the inner-shell electrons. The Fock matrix elements are as follows:

$$F_{ij} = h_{ij}^{V} + \sum_{l,m} P_{lm} \left[(ij|lm) \right] - \frac{1}{2}(im|lj) \tag{79}$$

There are a large number of semiempirical methods in use today such as MINDO/3, MNDO, AM1, PM3, PM5, and MNDO-*d* which have roughly the same structure. Semiempirical methods are thus seen to be well balanced: they are accurate enough to have useful predictive powers, yet fast enough to allow large systems to be studied. All the semiempirical methods contain sets of parameters.

MNDO method was modified based on the neglect of diatomic differential overlap (NDDO); this theory only neglects differential overlap between atomic orbitals on different atoms. The Austin Model 1 (AM1) and PM3 are based on MNDO (the name derives from the fact that PM3 is the third parametrization of MNDO, AM1 being considered the second). AM1 and PM3 modify the core-core repulsions just outside bonding distances. PM3 has two Gaussians per atom, while AM1 has two - four Gaussians per atom. In AM1 a sum of Gaussians is employed to better represent the core repulsion behaviour at van der Waals distances. PM3 uses a similar core repulsion function, but differs in the parameterisation procedure.

One advantage of methods parameterised using experimental data is their implicit inclusion of electron correlation effects. However, it must be kept in mind that these methods are parameterized for molecules in the ground state at 298 K. Therefore, the calculated results are dependent on experimental data. That means that semiempirical methods would not be expected to perform well on unusual types of molecules for which no experimental data are available, e.g. for systems far from their ground state equilibrium. In addition, the results from semiempirical methods should further be compared to the results of higher-level ab inito or density functional theory. Results are diffent for diffent methods. Some methods cannot calculate weak interaction like hydrogen bonding.

6. Molecular mechanics

Molecular mechanics (MM) methods, known as force field methods, are ideal for modelling such large systems. These methods employ a potential that ignores the electron distribution of a system and instead merely considers the positions of the nuclei within the system. The resulting potential energy function known as a force field is based on the interactions between the nuclei within the system and takes into account molecular processes.

Molecular mechanics force field are constructed and parameterized by comparison with a number of molecules. This force field then can be used for other molecules similar to those for which it was parameterized. To make a molecular mechanics calculation, a force field is chosen and suitable molecular structure values (natural bond lengths, angles, etc.) are set. The structure then is optimized by changing the structure incrementally to minimize the strain energy and spread it over the entire molecule. This minimization is orders of magnitude faster than a quantum mechanical calculation on an equivalent molecule so that it is reasonable to use molecular mechanics force field instead of quantum mechanical calculation for molecular dynamics simulations. Up to date, there are a number of different MM potentials that are in common use for biomolecular including the CHARMM, AMBER, GROMOS and OPLS potentials.

Molecular mechanics is a classical mechanical model that represents a molecule as a group of atoms held together by elastic bonds. Molecular mechanics looks at the bonds as springs which can be stretched called bond stretching. Compressed, bent at the bond angles, twisted in torsional angles and non-bonded interactions between atoms are also considered. The sum of all these forces is called the “force field” of the molecule. Many of the modeling force fields can be interpreted in terms of a relatively simple four component picture of the intra- and inter-molecular forces within the system. Energetic penalties are associated with the deviation of bonds and angles away from their reference and equilibrium values, there is a function that describes how the energy changes as bonds are rotated, and finally

the force field contains terms that describe the interaction between non-bonded parts of the system. More sophisticated force fields may have additional terms, but invariably contain these four components, so that it can be writing the general equation of the total energy of motion to be shown as:

$$V_{tot} = V_{bond} + V_{angle} + V_{torsion} + V_{vdw} + V_{elec} \quad (80)$$

6.1 Bonded interactions

Bonds stretching: The interaction between two atoms directly bonded to each other is assumed to be harmonic. Bond stretching energy can be represented as following,

$$E = \sum_{n=1}^{i} k_b (r - r_0)^2 \quad (81)$$

where r is the length of the ith bond (Å)
r_0 is the equilibrium length for the ith bond (Å)
k_b is the bond stretching constant (kcal/mol (Å)^2)

Bond angles: The interaction between three connected atoms is also assumed to be harmonic. Angle bending energy is a function of angular displacement. The bending energy equation is also based on Hooke's law

$$E = \sum_{n=1}^{i} k_\theta (\theta - \theta_0)^2 , \quad (82)$$

where θ is the angle between two adjacent bonds (degree)
θ_0 is the equilibrium value for the ith angle (degree)
k_θ is the angle bending constant (kcal/mol (degree)^2)

Dihedral (Torsion) angles: There are four atoms connected by three bonds, so that if we look straight down the second bond, the dihedral angle is the angle between the first and third bonds. The energies associated with dihedral angles are treated using a cosine series. The torsion energy is modeled by a simple periodic function.

$$E = \sum_{torsions} A\left[1 + Cos\left(n\tau - \phi\right)\right], \tag{83}$$

where A is the torsional barrier (kcal/mol)

$n\tau$ is the periodicity

ϕ is the torsional angle

6.2 Non-bonded interactions

The non-bonded energy represents the pair-wise sum of the energies of all possible interacting non-bonded atoms i and j;

$$E = \sum_i \sum_j \frac{-A_{ij}}{r_{ij}^6} + \frac{B_{ij}}{r_{ij}^{12}} + \sum_i \sum_j \frac{q_i q_j}{r_{ij}}, \tag{84}$$

where the first term of the right-hand side of the equation (84) is the Lennard-Jones potential energy function that represented the van der Waals attraction and repulsion between atom i and j. The second term is the electrostatic interaction between atom i and j.

Van der Waals attraction: Van der Waals attraction occurs at short range, and rapidly dies off as the interacting atoms move apart.

Repulsion: Repulsion occurs when the distance between interacting atoms becomes even slightly less than the sum of their contact distance.

Electrostatic interactions: Electrostatic energy dies out slowly and it can affect atoms quite far apart.

APPENDIX B: Presentations and Proceedings

Oral Presentation and Proceedings

1. Pensri Srivub, Mayuso Kuno, Peerapol Nunrium and Supa Hannongbua. **Theoretical Investigation on Binding Energy for Wild Type and Y181C Mutant HIV-1 RT/Efavirenz Complex, Based on ONIOM2 Method.** The 9th Annual National Symposium on Computational Science and Engineering (ANSCSE 2005), Faculty of Science, Mahidol University, Bangkok, Thailand, 25-27 March 2005.

Poster Contribution to Conferences

1. Pensri Srivub, Pornthip Boonsri, Peerapol Nunrium, Mayuso Kuno and Supa Hannongbua. **Different Interaction between Single Mutant and Double Mutant HIV-1 RT Complexed with Efavirenz Inhibitor; ONIOM Method.** Modeling Interactions in Biomolecules II, University of Agriculture in Prague, Prague, Czech, 5-9 September, 2005.

2. Pensri Srivub, Mayuso Kuno, Peerapol Nunrium, Pornthip Boonsri, Supa Hannongbua. **Theoretical Investigation on Binding Energy for wild type and Y181C mutant HIV-1 RT/efavirenz complex: quantum mechanics and ONIOM3 calculations.** International Conference on Modeling in Chemical and Biological Engineering Sciences (CBES2006), 26-27 October, 2006.

3. Suwipa Saen-oon, Mayuso Kuno, Peerapol Nunrium1, Pornthip Boonsri, Pensri Srivub1 and Supa Hannongbua**. Investigation on the Interaction between Non-Nucleoside inhibitors and Mutant HIV-1 Reverse Transcriptase (Y181C and K103N), Based on the Combined Quantum Mechanical Methods and Inhibitor Design.**

Different Interaction between Single Mutant and Double Mutant HIV-1 RT Complexed with Efavirenz Inhibitor ; ONIOM Method

Pensri Srivub*, Pornthip Boonsri, Peerapol Nunrium and Supa Hannongbua**
Chemistry Department, Faculty of Science, Kasetsart University, Bangkok, 10900 THAILAND.
g4684003@ku.ac.th* and fscisph@nontri.ku.ac.th**

Introduction

The human immunodeficiency virus type1 reverse transcriptase (HIV-1 RT) is essential enzyme in the life cycle of the virus and is an attractive target for the development of new drug. Efavirenz, a second generation non-nucleoside RT inhibitor (NNRTI), is one of the most potent and selective inhibitors with high activity against HIV-1 RT. Mutations of residues in binding pocket of RT reduce the sensitivity significantly. The most common RT mutation that confer resistance to NNRTIs such as K103N, Y181C. In order to understand the basis for the resilience of efavirenz against single mutation (K103N and Y181C) and double mutation (K103N/Y181C), therefore, quantum chemical calculations and two layered ONIOM method (ONIOM2) were applied to study the nature of particular interaction between efavirenz and the binding site of the HIV-1 RT.

Methodology

The model was obtained from crystal structure of efavirenz bound to HIV-1 RT for both K103N and Y181C mutant types from the Protein Data Bank with the PDB entry codes 1IKV and 1JKH, respectively. Whereas the double mutant type was modeled from PDB entry code 1IKV by replacing tyrosine 181 with cysteine 181 to generate K103N/Y181C mutant type. The system was adopted by consisting of 22 amino acid residues concerted at efavirenz which assumed to be in their neutral form, see Fig. 2. All amino acids were terminated by capping with CH_3COO- and -$NHCH_3$ at the N- and at the C-terminals with their bonds and torsion angles assumed to be the same as in X-ray structure. Hydrogen atoms were added to generate the completed structure of the model and their positions were optimized with semiempirical method (PM3). These structures were used as the starting geometry for all calculations.

Interaction energy calculations

The interaction energy (INT) between efavirenz inhibitor and the individual residues were determined by quantum chemical calculations at B3LYP/6-31g(d) level of theory which is defined in Eq. (1).

$$INT_{(EFV-Xi)} = E_{(EFV-Xi)} - E_{EFV} - E_{Xi} \quad (1)$$

Where : INT is the interaction energy
X_i is the individual residues, EFZ is efavirenz inhibitor

ONIOM calculations

Two layered ONIOM2 was used to investigate interaction between efavirenz and residues in the HIV-1 RT binding site as shown in Fig. 2. In the ONIOM2 method, the system was divided into two parts. The inner layer (region A) was treated at B3LYP/6-31g(d) and HF/6-31g(d), and remaining (region B) was treated at PM3 level of calculations. During optimization backbone were fixed as in the X-ray structure. Binding energy calculations of efavirenz bound to the HIV-1 RT binding pocket was also performed using the ONIOM2 method and definition can be expressed by Eq. (2).

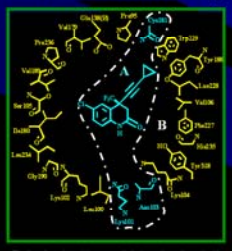

Fig. 2. Adopted model system of efavirenz bound to double mutant of HIV-1 RT binding site consisting of 22 amino acid residues. Layer partitioning is shown for ONIOM2 [A is the inner layer, and B is the outer layer].

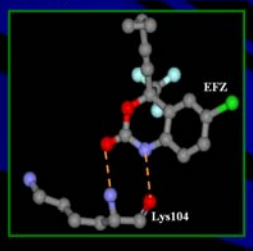

Fig. 3. Both of hydrogen bonding interaction between benzoxazine-2-one(NH and –C=O) and the backbone carbonyl (C=O) and backbone amino hydrogen (NH) of K101for HIV-1 RT

Discussion

The interaction between efavirenz and Lys101 is the strongest interaction, which is the main contributor for both single- and double mutant systems as shown in Table 1. The interaction between efavirenz and K101 can exhibit moderate hydrogen bonding between benzoxine-2-one (-NH and –C=O) and the backbone carbonyl oxygen (C=O) of Lys101 and backbone amino hydrogen (-NH) of Lys101 as shown in Fig 3. Moreover, the interactions of efavirenz with residues surrounding the binding pocket of the single mutant type are more attractive than the double mutant type. The ONIOM2 calculations were carried out to determine the binding energies of efzvirenz bound into the HIV-1 RT binding pocket. The combinations of B3LYP/6-31G(d):PM3 and HF/6-31G(d):PM3 methods were performed. The binding energies of efavirenz in the binding pocket of HIV-1 RT come from ΔE (High, A), the interaction energy in the region A and ΔΔE (low, AB-A), the interaction energy between the regions A and B as shown in Table 2. It is found that ΔΔE (low, AB-A) for the single- and double mutant types are not significantly different. The main difference energy was obtained from interaction in region A. This results come from the effect of mutation from Lys103 to Asn103 which is unfavorable surface contact as shown in Fig. 1.

Results

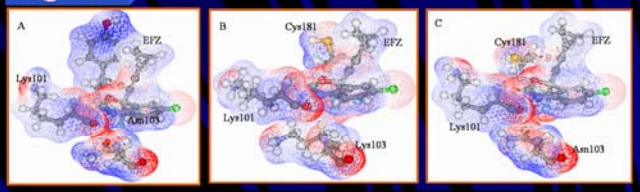

Fig. 1. Electrostatic potential of solvent accessible surface as red for negative and blue for positive values for efavirenz bound to K103N(A), Y181C(B), K103N/Y181C(C).

Table 1. Interaction energies of efavirenz with individual residues (in kcal/mol), calculate at the B3LYP/6-31G(d) level of theory

Residue	Interaction energy (kcal/mol)			
	Wild type*	K103N mutant	Y181C mutant	K103N/Y181C mutant
Pro95	-0.35	-0.37	-0.15	-0.27
Leu100	-3.98	0.17	0.61	2.19
Lys101	**-11.29**	**-8.96**	**-12.59**	**-7.2**
Lys102	1.46	0.58	1.04	0.53
Lys103(Asn)	-1.53	(-1.08)	-0.62	(-0.98)
Lys104	-0.09	0.03	0.12	-0.16
Ser105	-2.33	0.35	0.14	0.36
Val106	1.01	0.74	0.26	2.03
Val179	1.34	-1.72	-1.55	0.86
Ile180	-0.39	-0.16	-0.08	-0.15
Tyr181(Cys)	-0.38	1.02	(1.38)	(-0.23)
Tyr188	-1.09	-0.39	-0.19	1.72
Val189	-1.90	-0.51	-0.62	-0.25
Gly190	-0.49	-0.82	-1.1	0.19
Phe227	-0.06	0.3	-0.11	0.51
Leu228	0.13	0.02	-0.16	0.02
Trp229	-0.23	1.58	-1.04	2.01
Leu234	0.19	1.52	1.3	3.58
His235	-2.24	-0.93	-2.16	-0.48
Pro236	-1.72	0.57	0.29	0.97
Tyr318	-0.27	-0.85	-0.55	-0.44
Glu138	1.46	0.06	0.65	0.11
Total	-22.66	-9.58	-17.9	-7.19

*From Ref.4

Table 2. Comparison of binding energy between the single- (Y181C, K103N) and double mutant type (Y181C/K103N) HIV-1 RT, complexed with efavirenz, calculated by different ONIOM models.

Methods	Systems	Calculate energies (kcal/mol)		
		ΔE	ΔE(High, A)	ΔΔE (Low,AB-A)
ONIOM2A	K103N	-12.35	-5.10	-7.25
HF/6-31G(d):PM3	Y181C	-13.54	-7.49	-6.04
	K103C/Y181C	-12.03	-4.29	-7.74
ONIOM2B	K103N	-13.35	-5.85	-7.50
B3lyp/6-31G(d):PM3	Y181C	-15.01	-8.60	-6.41
	K103C/Y181C	-12.20	-4.10	-8.10

$$\Delta E^{ONIOM2} = E \text{ (optimized complex)} - E \text{ (optimized pocket)} - [E \text{ (optimized efavirenz)}] \quad (2)$$
$$= \Delta E \text{ (High, A)} + [\Delta E \text{ (Low, AB)-}\Delta E \text{ (Low, A)}]$$
$$= \Delta E \text{ (High, A)} + [\Delta\Delta E\text{(Low, AB-A)}]$$

Where : ΔE (High, A) is the interaction energy in the region A ,
ΔΔE (low, AB-A) is the interaction energy between the regions A and B evaluated at the low level.

Conclusions

1. The interaction between efavirenz and Lys101 is the strongest interaction, which is the main contributor for both of the wild type and mutant systems.
2. The main difference energy was obtained from interaction in region A. This results come from the effect of mutation from Lys103 to Asn103 which is unfavorable surface contact, therefore, efavirenz drop inhibiting efficiency against the K103N and K103N/Y181C of HIV-1 RT. Finally, efavirenz is higher inhibitory affinity against Y181C mutation

Acknowledgements

- Thailand Research Fund (TRF) and Commission for Higher Education
- Postgraduate on Education and Research in Petroleum and Petrochemical Technology (MUA-ADB)
- Kasetsart University Research and Development Institute (KURDI)
- LCAC and computing centers of KU
- Rajamangala University of Technology Sivijaya.

References

1. J. Ren, C. Nichols, L. Bird, P. Chamberlain, K. Weaver, S. Short, D. I. Stuart and D. K. Stammers, *J. Mol. Bio.* 312 (2001) 795.
2. M.Udier-Blagovi , E. K. Watkins, J. Tirado-Rives and W. L. Jorgensen, *J. Med. Chem.* 47 (2004) 2389.
3. M. Kuno, S. Hannongbua and K. Morokuma, *Chem. Phy. Lett.* 380 (2003) 456.
4. P. Nunrium, M. Kuno, S. Saen-oon and S. Hannongbua, *Chem. Phy. Lett.* 405 (2005) 198.

Theoretical Investigation on Binding Energy for Wild Type and Y181C Mutant HIV-1 RT/Efavirenz Complex using Quantum Mechanics and ONIOM Calculations

Pensri Srivub[1], Mayuso Kuno[2], Pornthip Boonsri, Peerapol Nunrium and Supa Hannongbua[1]*

[1]Chemistry Department, Faculty of Science, Kasetsart University, Bangkok, 10900 THAILAND.
[2]Current address: Department of Chemistry, Faculty of Science, Srinakharinwirot University, Sukhumvit 23, Bangkok, 10110, Thailand
g46f4003@ku.ac.th and fscisph@mozart.ku.ac.th

Introduction

The human immunodeficiency virus type1 reverse transcriptase (HIV-1 RT), which is an essential enzyme in the life cycle of the virus, is an attractive target for the development of new drugs. Efavirenz is a non-nucleoside RT inhibitor (NNRTI) which has high activity against HIV-1 RT. However, the efficacy of highly potent NNRTIs is limited by drug-resistant mutant. The Y181C mutation is the most common HIV-1 RT mutation associated with resistance to NNRTIs. In order to understand the basis for the resilience of the efavirenz at molecular level and to help the design of further improved anti-AID agents, ONIOM method was applied to study the nature of particular interactions between the efavirenz and binding site of the HIV-1 RT[1,2,3]

Methodology

The model was obtained from crystal structure of efavirenz bound to HIV-1 RT [(Wild type; 1FK9), (Y181C; 1JKH)]. The system was adopted consisting of 22 residues concerted at efavirenz which was assumed that their neutral forms (Figure 2). All amino acids were terminated by capping with an acetyl group(CH_3CO-) and a methyl amino group (-$NHCH_3$) at the N- and C-terminals, respectively (Figure 1). Their bonds and torsion angles were assumed to be same as X-ray structure. Hydrogen atoms were added to generate the completed structure of the model and their positions were optimized with semi-empirical method (PM3). These structures were used as the starting geometry for all calculations. The interaction energy (INT) between efavirenz and the individual residues was determined by using quantum chemical calculations at B3LYP/6-31G(d,p) and MP2/6-31G(d,p) level of theory which is defined in equation (1).

$$INT_{(EFV+Xi)} = E_{(EFV+Xi)} - E_{EFV} - E_{Xi} \quad \cdots (1)$$

where: INT is the interaction energy.
Xi is the individual residues, EFV is Efavirenz inhibitor.

ONIOM Calculations

Calculated Binding energies of efavirenz bound to the HIV-1 RT binding pocket were performed using three-layer ONIOM calculations. On the basis of ONIOM method shown in scheme 1, the total energy of the entire system was obtained from three and five independent energy calculations in ONIOM2 and ONIOM3 methods as following equation (2) and (4), respectively. The binding energy of efavirenz bound to its binding pocket of HIV-1 RT was calculated with various combined two- and three-layers ONIOM methods are defined as following equation (6) and (7). Partial optimization was performed by fixing the heavy atoms to represent the real structure from X-ray.

Fig. 1. Capped groups of the N- and C-terminal ends for amino acid chain

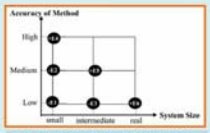

Scheme 1. Schematic representation of the three-layer ONIOM extrapolation

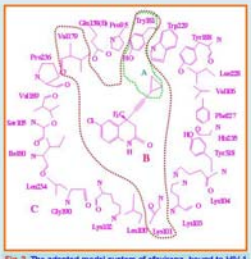

Fig. 2. The adopted model system of efavirenz bound to HIV-1 RT binding site consisting of 22 amino acid residues. Layer partitioning is shown for ONIOM3 method [A is the inner layer, B is the medium layer and C is the outer layer]

$$E^{ONIOM2} = E(low,real) - E(low,small) + E(high,small) \quad \ldots (2)$$

or $E^{ONIOM2} = E6 - E1 + E4 \quad \ldots (3)$

$$E^{ONIOM3} = E(low,real) - E(low,int) + E(medium,int) - E(medium,small) + E(high,small) \quad \ldots (4)$$

or $E^{ONIOM3} = E6 - E3 + E5 - E2 + E4 \quad \ldots (5)$

ONIOM2:
ONIOM2A: HF/6-31G(d,p)[EFZ+K101+ V179 + Y181]: PM3[real]

ONIOM2B: B3LYP/6-31G(d,p)[EFZ+K101+V179 + Y181]: PM3[real]

ONIOM3:
ONIOM3A: B3LYP/6-31G(d,p)[EFZ +Y181]: HF/6 31G(d,p)[EFZ+K101+ V179]: PM3[real]

ONIOM3B: MP2/6-31G(d,p)[EFZ+Y181]: HF/6-31G(d,p)[EFZ+K101+ V179 + Y181]: PM3[real]

ONIOM3C: MP2/6-31G(d,p)[EFZ+Y181]: B3LYP/631G(d,p)[EFZ+ K101+ V179 +Y181]: PM3[real]

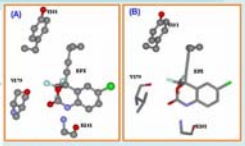

Fig 3. Presented (A) the components in small model for two-layer ONIOM model. (B) the three-layer ONIOM models, the components in intermediate model and the selected part of molecule for small model are represented with ball-and-stick style.

Results

Table1. Interaction energies of efavirenz with individual residues (Xi) calculated by B3LYP/6-31G(d,p) and MP2/6-31G(d,p) methods (in kcal/mol)

	Interaction Energy (kcal/mol)					
	B3LYP/6-31G(d,p)			MP2/6-31G(d,p)		
Residue	Wild type	Y181C	ΔE_{int}	Wild type	Y181C	ΔE_{int}
Pro95	-0.33	-0.13	-0.20	-1.09	-0.91	-0.18
Leu100	-0.56	0.59	-1.13	-7.06	-7.68	0.62
Lys101	-12.49	-12.68	0.19	-14.81	-15.00	0.19
Lys102	1.01	1.05	-0.04	0.17	0.11	0.06
Lys103	-1.08	-0.65	-0.43	-5.15	-3.87	-1.28
Lys104	0.11	0.11	-0.01	0.04	0.05	-0.01
Ser105	0.06	0.14	-0.08	-0.06	0.01	-0.07
Val106	1.08	0.24	0.84	-2.89	-3.90	1.01
Val179	1.61	-1.87	3.18	0.96	-2.84	2.90
Ile180	-0.17	-0.09	-0.08	-0.50	-0.32	-0.18
Tyr181(Cys)	-0.28	(-1.28)	1.12	-2.87	(-3.86)	-0.31
Tyr188	-1.14	-0.26	-0.88	-6.21	-6.67	0.46
Val189	-0.49	-0.62	0.13	-1.09	-1.31	0.22
Gly190	-1.60	-1.15	0.12	-1.75	-1.97	0.22
Phe227	0.07	-0.12	0.19	-1.04	-1.24	0.20
Leu228	-0.06	-0.16	0.10	-0.08	-0.18	0.10
Trp229	-0.86	-1.07	0.21	-3.24	-4.13	0.90
Leu234	0.15	1.28	-1.13	-1.96	-1.53	-0.43
His235	-1.58	-2.21	0.63	-2.87	-3.43	0.56
Pro236	-0.56	0.23	-0.78	-2.81	-1.81	-1.01
Tyr318	-0.37	-0.54	0.17	-2.87	-3.51	0.65
Glu138	1.83	0.61	1.22	1.26	-0.22	1.48

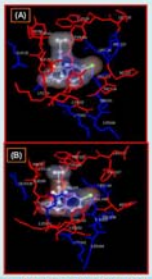

Fig. 4. Attractive interactions (red) and repulsive interactions (blue) of efavirenz with individual residue (Xi) (A) wild type and (B) Y181C mutant type.

$$\Delta E_{INT} = E_{(EFV+Xi)} - E_{(EFV+Xi)=0} + E_{EFV=0} - E_{EFV}$$

Table 2. Comparison of binding energy between the wild type and Y181C mutant type of HIV-1 RT, complexed with efavirenz, calculated by different ONIOM models.

		Calculate energies (kcal/mol)			
Methods	Systems	ΔE	ΔE(High, A)	$\Delta\Delta E$ (Mid,AB-A)	$\Delta\Delta E$ (Low,ABC-AB)
ONIOM2A HF/6-31G(d,p):PM3	Wild type	-17.46	-9.55	-	-7.91
	Y181C	-17.45	-8.56	-	-8.89
ONIOM2B B3lyp/6-31G(d,p):PM3	Wild type	-19.69	-10.21	-	-8.48
	Y181C	-19.25	-8.56	-	-9.69
ONIOM3A B3lyp/6-31G(d,p):HF/6-31G(d,p):PM3	Wild type	-18.68	0.26	-10.12	-8.82
	Y181C	-17.75	1.44	-10.00	-9.19
ONIOM3B MP2/6-31G(d,p):HF/6-31G(d,p):PM3	Wild type	-19.36	-0.85	-10.33	-8.28
	Y181C	-18.45	0.81	-10.04	-9.22
ONIOM3C MP2/6-31G(d,p):B3LYP/6-31G(d,p):PM3	Wild type	-20.52	-0.82	-11.02	-8.69
	Y181C	-19.49	0.86	-10.79	-9.56
Experiment binding loss		2.5 fold			

$$\Delta E^{ONIOM2} = E[Cpx]opt - E[P]opt - E[L]opt$$
$$= \Delta E\,(High, AB) + [\Delta E\,(Low, ABC) - \Delta E\,(Low, AB)]$$
$$= \Delta E\,(High, AB) + [\Delta\Delta E(Low, ABC\text{-}AB)] \quad \ldots (6)$$

$$\Delta E^{ONIOM3} = E[Cpx]opt - E[P]opt - E[L]opt$$
$$= \Delta E\,(High, A) + [\Delta E\,(Mid, AB) - \Delta E\,(Mid, A)] + [\Delta E\,(Low, ABC) - \Delta E\,(Low, AB)]$$
$$= \Delta E\,(High, A) + [\Delta\Delta E(Mid, AB\text{-}A)] + [\Delta\Delta E(Low, ABC\text{-}AB)] \quad \ldots (7)$$

Where : ΔE (High, A) is the interaction energy in the region A.
$\Delta\Delta E$ (Mid, AB-A) is the interaction energy between the regions A and B evaluated at the low level.
$\Delta\Delta E$(Low, ABC-AB)] is the interaction energy between the regions AB and C.

Discussion

Fig. 4 shows the graphical presentation of the attractive and repulsive interactions. It is clearly seen that there are more attractive interactions between efavirenz and the residues surrounding the binding site of the HIV-1 RT for both wild type and Y181C mutant type. Interactions between efavirenz and residues in binding pocket of HIV-1 RT for both wild type and Y181C mutant type are different only Valine with position at 179 as shown in Table 1. Particularly, the interaction between efavirenz and K101 for both the wild type and Y181C mutant type were calculated at MP2/6-31(d,p) levels and it shows the strongest interaction, -15 kcal/mol. Binding energy difference between wild type and Y181C mutant type for all ONIOM3 calculations is 1 kcal/mol. The mutation of Y181 to smaller non-aromatic side chain cysteine does not have much effect on binding of efavirenz to the binding pocket of HIV-1 RT.

Conclusions

The binding energy difference between the wild type and its Y181C mutant complexes are approximately 1 kcal/mol. Additionally, Interactions between efavirenz and residues in the binding pocket of HIV-1 RT for both wild type and Y181C mutant type are different only at V179. In summary, efavirenz is high inhibitory affinity against for both the wild type and Y181 mutant type.

Acknowledgements

- Thailand Research Fund (TRF) and Education and Research on Petroleum and petrochemical Technology (MUA-ADB)
- Center of Nanotechnology Kasetsart University Research and Development Institute (KURDI)
- LCAC and computing center of KU for research facilities.
- Rajamangala University of Technology Sivijaya.

References

1. Kuno, M., Hannongbua, S. and Morokuma,K., Theoretical Investigation on Nevirapine and HIV-1 Reverse Transcriptase Binding Site Interaction, Based on ONIOM Method *Chem. Phy. Lett.* 380 (2003) 456.
2. Nunrium, P., Kuno, M., Saen-oon, S. and Hannongbua, S., Particular Interaction between Efavirenz and the HIV-1 RT binding site as explained by the ONIOM2 method, *Chem. Phy. Lett.* 405 (2005) 198.
3. Saen-oon, S., Kuno, M., and Hannongbua, S., Binding Energy Analysis for Wild type and Y181C Mutant HIV-1 RT9-Cl TIBO Complex Structures: Quantum Chemical Calculations, Based on ONIOM Method, *PROTEINS: Structure, Function, and Bioinformatics* 61 (2005) 859.

Investigation on the Interaction between Non-Nucleoside inhibitors and Mutant HIV-1 Reverse Transcriptase (Y181C and K103N), Based on the Combined Quantum Mechanical Methods and Inhibitor Design

Suwipa Saen-oon[1,2], Mayuso Kuno[1,3], Peerapol Nunrium[1], Pornthip Boonsri[1], Pensri Srivub[1] and Supa Hannongbua[1]*

[1]Chemistry Department, Faculty of Science, Kasetsart University, Bangkok, 10900 THAILAND
[2]Current address: Chemistry Department, Emory University, Atlanta, GA, 30322, USA
[3]Current address: Department of Chemistry, Faculty of Science, Srinakharinwirot University, Sukhumvit 23, Bangkok, 10110, Thailand
*Corresponding author Tel.: +66-2-9428900 ext 217; Fax : +66-2-9428900 ext 218; Email : fscisph@ku.ac.th.

Introduction

The human immunodeficiency virus type1 reverse transcriptase (HIV-1 RT) is essential enzyme in the life cycle of the virus and is an attractive target for the development of new drug. Efavirenz and TIBO are non-nucleoside RT inhibitor (NNRTI) with high activity against HIV-1 R. However, the efficacy of these highly potent inhibitors is limited by drug-resistant mutants. The most common HIV-1 RT mutations associated with resistance to NNRTIs are the Lys103Asn (K103N) and Tyr181Cys (Y181C) substitutions. In order to understand the basis for the resilience of these inhibitors at molecular level and to help the design of further improved anti-AID agents therefore, combined quantum chemical calculations or ONIOM method were applied to study the nature of particular interaction between these inhibitors and the binding site of the HIV-1 RT.

Methodology

The model were obtained from crystal structure of efavirenz and TIBO bound to HIV-1 RT for both wild-type, mutant types (Y181C and K103N). The system of interest for the investigation of interactions between these inhibitors in the binding pocket of the RT were well defined for both the wild-type and mutant type which assumed to be in their neutral form, see Fig. 2 and 3. All amino acids were terminated by capping with CH_3COO- and -$NHCH_3$ at the N- and at the C-terminals (Fig 1.), which their bonds and torsion angles assumed to be the same as in X-ray structure. Hydrogen atoms were added to generate the completed structure of the model and their positions were optimized with semiempirical method (PM3). These structures were used as the starting geometry for all calculations. The interaction energy (INT) between theses inhibitors and the individual residues were determined by quantum chemical calculations at B3LYP/6-31g(d) and MP2/6-31g(d) level of theory. Binding energy calculations of efavirenz and TIBO bound to the HIV-1 RT binding pocket were performed using two- and three-layer ONIOM calculations (ONIOM2 and ONIOM3). ONIOM2 focused on the direct interaction between these inhibitors and residues Y181C or/and K103N in the HIV-1 RT binding site. To include more important distribution to the binding interactics, the three-layered ONIOM3 was then applied. The high level of theory calculations was used by the HF, B3LYP and MP2 methods and semiempirical (PM3) method was used as the low level of theory to treat the real system. The system was divided into two parts. During optimization backbone were fixed as in the X-ray structure.

Results

Table 1. Interaction energies of efavirenz and TIBO with individual residues (in kcal/mol), calculate at the B3LYP/6-31G(d) and MP2/6-31g(d) level of theory

	Interaction energy of efavirenz with individual residues (kcal/mol)						Interaction energy of TIBO with individual residues(kcal/mol)			
	B3LYP/6-31g(d)			MP2/6-31g(d)			B3LYP/6-31g(d,p)		MP2/6-31g(d,p)	
Residue(X_i)	Wild type*	K103N	Y181C	Wild type*	K103N	Y181C	Wild type	Y181C	Wild type	Y181C
Pro95	-0.08	-0.16	0.06	-0.68	-0.78	0.17	0.27	3.82	-1.19	1.79
Leu100	2.31	2.82	3.78	-2.98	-1.79	-2.23	1.67	7.26	-4.79	-0.84
Lys101	-8.12	-6.59	-8.10	-9.22	-7.45	-9.15	-10.83	-11.96	-13.22	-14.80
Lys102	1.21	0.83	1.24	0.53	0.08	0.49	0.97	0.77	0.27	0.18
Lys103(Asn)	1.32	(2.15)	1.32	-1.69	(-0.57)	-1.19	1.36	0.73	-1.76	-1.83
Lys104	0.11	0.00	0.12	0.05	-0.10	0.06	-	-	-	-
Ser105	0.06	0.36	0.14	-0.05	0.23	0.02	-	-	-	-
Val106	2.14	2.43	1.86	-0.29	-0.47	-0.87	1.46	2.38	-2.45	-1.43
Val179	4.19	1.10	0.02	3.20	-0.23	-1.17	1.39	-0.67	-1.21	-2.05
Ile180	-0.12	-0.15	-0.07	-0.44	-0.36	-0.30	-0.20	-0.17	-1.36	-1.27
Tyr181(Cys)	1.02	2.35	(-0.31)	-1.78	-0.09	(-2.22)	0.23	(3.40)	-3.37	(-0.26)
Tyr188	1.71	2.79	3.26	-2.57	-1.32	-1.77	3.28	4.65	-3.36	-1.86
Val189	-0.12	-0.15	-0.12	5.08	-0.76	-0.78	0.06	0.16	-0.69	-0.34
Gly190	0.54	0.45	0.83	-0.10	-0.12	0.15	-0.12	-0.08	-1.16	-0.65
Phe227	0.34	0.87	0.20	-0.45	-0.06	-0.66	2.31	-0.02	-0.16	-1.19
Leu228	-0.06	0.02	-0.16	-0.08	-0.02	-0.18	0.06	0.03	-0.07	-0.07
Trp229	-0.05	3.10	0.06	-2.04	-0.90	-2.28	0.49	2.79	-3.34	-1.32
Leu234	0.93	2.67	2.27	-0.58	0.37	0.59	2.36	-0.04	-0.15	-1.34
His235	0.40	0.66	-0.39	-0.56	-0.34	-1.36	-2.41	-0.37	-4.01	-1.05
Pro236	1.07	1.59	1.37	-0.37	0.44	0.13	-0.43	-0.85	-1.97	-2.20
Tyr318	0.51	0.37	0.64	-1.68	-1.94	-1.84	-1.57	2.05	-4.52	-0.20
Gln338	1.88	0.05	1.29	1.37	-0.14	0.56	0.53	-0.10	0.19	-0.88

$INT_{inhibitor+Xi} = E_{inhibitor+Xi} + E_{inhibitor} - E_{Xi}$

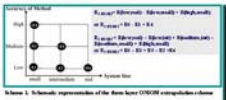

Scheme 1. Schematic representation of the three layer ONIOM extrapolation scheme

Fig. 1. Capped groups of the N- and C-terminal ends for amino acid chain.

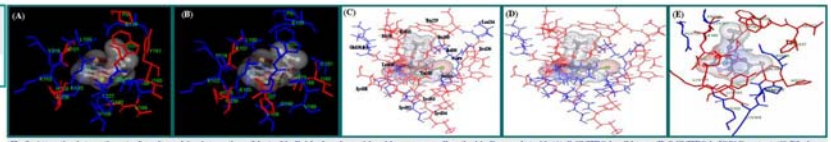

Fig 5. Attractive interactions (red) and repulsive interactions (blue) of individual amino acid residues, surrounding the binding pocket with (A) S-Cl TIBO in wild type, (B) S-Cl TIBO in Y181C mutant, (C) Efavirenz in wild type, (D) Efavirenz in K101E mutant and (E) Efavirenz in Y181C mutant HIV-1 RT.

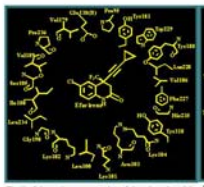

Fig. 2. Schematic representation of the adopted model system of efavirenz bound to the HIV-1 RT binding site

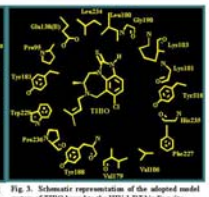

Fig. 3. Schematic representation of the adopted model system of TIBO bound to the HIV-1 RT binding site

Table 2. The BE With BSSE Correction for the TIBO and HIV-1 RT Complex by Various ONIOM2 and ONIOM3 Methods

Methods	BE (kcal/mol)		
	Wild- type	Y181C mutant	[b]ABE
ONIOM2A* B3LYP/6-31G(d,p):PM3	-13.90	-8.54	-5.36
ONIOM2B B3LYP/6-31G(d,p):PM3	-13.59	-4.33	-9.26
ONIOM3C MP2/6-31G(d):B3LYP/6-31G(d,p):PM3	-13.88	-4.65	-9.23
ONIOM3D B3LYP/6-31G(d):HF/6-31G(d,p):PM3	-12.76	-4.96	-7.80

Table 3. The BE With BSSE Correction for the efavirenz and HIV-1 RT Complex by ONIOM2 Method

Methods	BE (kcal/mol)		
	Wild- type*	Y181C mutant	K103N mutant
ONIOM2A B3LYP/6-31G(d,p):[EFZ+E101+(Y181 or C181)+(K103 or N103)]: PM3[rest]	-16.72	-13.54	-12.35
ONIOM2B B3LYP/6-31G(d,p):EFZ+E101+(Y181 or C181)+ (K103+N103)]: PM3[rest]	-20.06	-15.01	-13.35

*Non-BSSE correction. [b]$ABE = BE_{wild\ type} - BE_{Y181C\ mutant}$

$BE_{ONIOM} = E(Inhibitor + HIV\text{-}1\ RT)_{opt} - E(HIV\text{-}1\ RT)_{opt} - E(Inhibitor)_{opt}$

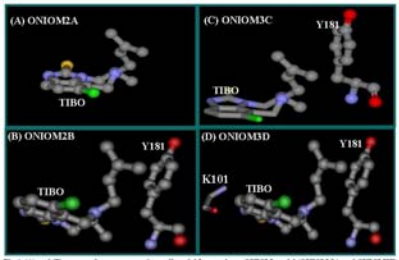

Fig 4. (A) and (B) present the components in small model for two-layer ONIOM model (ONIOM 2A and ONIOM2B). (C) and (D), which are for the three-layer ONIOM models (ONIOM3C and ONIOM3D), present the components in intermediate model and the selected part of molecule for small model are represented with ball-and-stick style.

Discussion

Two- and three-layer ONIOM calculations were applied to determine the BE of TIBO to the HIV-1 RT binding pocket of both wild-type and Y181C mutant type. These results clearly show that the mutation of Y181C as compared with the wild type decreases the stabilization energy of TIBO binding to its binding pocket. Comparison of the complex structures suggests that the Y181C mutation eliminates favorable contacts of the aromatic ring of the tyrosine and the bound inhibitor, reducing the stability of TIBO binding. Clearly, there are more repulsive interactions between TIBO with residue surrounding the binding pocket. For binding energy of efavirenz, comparison between wild type and mutant type (K103N, Y181C) was performed by using two-layered ONIOM method. The results clearly show that two major mutants, K103N and Y181C as compared to the wild type decrease the stabilization energy of efavirenz binding to its binding pocket. In K103N mutant , the replacement of Lys103 by Asn103 creates a small repulsion between efavirenz and Asn103. The interaction between these inhibitors and lys101 is the strongest interaction, which is the main contributor for both wild type and mutant type as shown in Table 1.

Conclusions

1. The binding energies of efavirenz and TIBO to binding pocket in mutants (K103N or Y181C) as compared to the wild type decrease the stabilization energies of these inhibitors binding to their binding pockets.
2. The interaction of TIBO and efavirenz inhibitors with lys101 is the strongest interaction for both wild type and mutant type.

Acknowledgements

- Thailand Research Fund (TRF) .
- Postgraduate on Education and Research in Petroleum and Petrochemical Technology (MUA-ADB)
- Kasetsart University Research and Development Institute (KURDI)
- LCAC and computing centers of KU

References

1. Kuno, M., Hannongbua, S. and Morokuma,K., Theoretical Investigation on Nevirapine and HIV-1 Reverse Transcriptase Binding Site Interaction, Based on ONIOM Method *Chem. Phy. Lett.* 380 (2003) 456.
2. Nunrium, P., Kuno, M., Saen-oon, S. and Hannongbua, S., Particular Interaction between Efavirenz and the HIV-1 RT binding site as explained by the ONIOM2 method, *Chem. Phy. Lett.* 405 (2005) 198.
3. Saen-oon, S., Kuno, M., and Hannongbua, S., Binding Energy Analysis for Wild type and Y181C Mutant HIV-1 RT/8-Cl TIBO Complex Structures; Quantum Chemical Calculations, Based on ONIOM Method, *PROTEINS*, (2005), inpress.

Pensri Srivub

Laboratory for Computational and Applied Chemistry
Department of Chemistry, Faculty of Science, Kasetsart University
50 Pahonyothin Road, Lat Yao Subdistrict, Jatujak District, Bangkok, THAILAND
10900.

PERSONAL DETAILS

Date of Birth:	10th June 1970
Place of Birth:	Songkla, Thailand
Nationality:	Thai
Marital Status:	Single
Age:	37
Phone Number:	+66-2942-8900 ext.325
Fax Number:	+66-2942-8900 ext.324
E-mail address:	g4684003@ku.ac.th, pensri_srivub@yahoo.com

EDUCATION

Kasetsart University, Bangkok, Thailand

- Ph.D. in Physical Chemistry 2003-Present

King Mongkut's Institue of Technology North Bangkok, Thailand

- Ms in Industrial Chemistry 1996-1999

Pince of Songkla University, Thailand

- B.Sc. in Chemistry 1989-1993

RESEARCH VISITING

University of Vienna, Austrial

- Research work with Prof. Dr. Peter Wolschann 5 Feb. 2007 – 5 April 2007

Research Assistant (2003- present)
Laboratory for Computational and Applied Chemistry Physical Chemistry Division, Kasetsart University, Bangkok, Thailand

RESEARCH INTERESTS

- Particular interactions between inhibitor and its binding pocket of HIV-1 Reverse Transcriptase using quamtum mechanics calculation and ONIOM method
- Molecular dynamics simulation in biomolecular systems

PUBLICATIONS

1. Understanding on Different Binding Energies of Efavirenz to Wild Type and K103N/Y181C HIV-1 Reverse Transcriptase, Based on ONIOM Method Pensri Srivub and Supa Hannongbua. Submited.

2. Study of the NNRTIs binding to double mutant K103N/Y181C HIV-1 RT using combined ONIOM quantum chemical-molecular dynamics. Pensri Srivub, Anton Beyer, Supa Hannongbua, Peter Wolschann. in preparation.